Supplementary Material to:

Translational predictions of phase 2a first-in-patient efficacy studies for antituberculosis drugs

Jacqueline P. Ernest[1†], Janice Jia Ni Goh [1†], Natasha Strydom[1†], Qianwen Wang[1†], Rob C. van Wijk [1†], Nan Zhang[1†], Amelia Deitchman[1], Eric Nuermberger[2], Rada M. Savic[1*]

Affiliation:

[1]Department of Bioengineering and Therapeutic Sciences, University of California, San Francisco, San Francisco, California, United States of America

[2]Center for Tuberculosis Research, Department of Medicine, Johns Hopkins University School of Medicine, Baltimore, Maryland, United States of America

[†]Shared authorship ordered alphabetically

[*]Corresponding author

Address:

1700 4th St, Rm 503C

University of California, San Francisco Box 2552

San Francisco, CA 94158, United States

Telephone number: +1 415 502-0640

E-mail address: rada.savic@ucsf.edu

Supplemental Methods

Study design

This translational platform is designed to understand the PK/PD relationships of TB drugs in murine TB model and extrapolate the findings to predict the clinical outcomes of phase 2a studies (Figure 1). Ten drugs were included: bedaquiline (BDQ), delamanid (DLM), ethambutol (EMB), isoniazid (INH), linezolid (LZD), moxifloxacin (MXF), pretomanid (PMD), pyrazinamide (PZA), rifampin (RIF), and rifapentine (RPT). A baseline model using the preclinical data in murine TB model was established previously to quantitate the inhibitory effect of the adaptive immune response on bacterial growth, and a net drug effect can therefore be quantified to establish the PK/PD relationships for the experimental regimens in mice. It was assumed at the free drug concentration level in blood, the PK/PD relationships of TB drugs are comparable between mice and humans. As such, with simulated PK concentrations in humans, the corresponding drug effect of TB drugs in humans can be predicted using the same PK/PD relationships as in mice, as well as the clinical outcome of TB monotherapy regimens in phase 2a trials.

Database

The sources for all data involved in the translational platform development are listed in **Table S1**. Preclinical plasma PK concentrations and lung CFU counts as PD data of BDQ, DLM, EMB, INH, LZD, MXF, PMD, PZA, RIF and RPT were collected from published and unpublished studies or digitized from published studies using Plot Digitizer (http://plotdigitizer.sourceforge.net/). Subacute infection data was used for all drugs except EMB, RPT and LZD for which data from the subacute infection model were not available. Clinical PK data were simulated using published human population PK models or models developed internally.

CFU counts in sputum samples for the nine drugs were collected or digitized from published clinical studies.

Model development

All analyses were conducted using NONMEM (version 7.4). Perl speaks NONMEM (PsN, 4.8.1), R (version 4.1.3) statistical program, and the xpose4 and tidyverse R packages were utilized for model diagnostics and data visualization. The first-order conditional estimation with interaction method (FOCE+I) was used. Mouse PK and PK/PD models were developed and selected based on graphical (goodness of fit plots), statistical (significant change in objective function value), and simulation-based diagnostics (visual predictive checks).

Mouse PK models for all drugs except EMB for which no PK data was available,were developed by fitting the plasma concentration data to one- or two-compartment structural models with first-order absorption and linear or nonlinear (Michaelis-Menten) clearance. Saturable bioavailability was also tested. Additive, proportional, and combination residual error models were tested to describe the error in the observed data (Figure S1). An EMB mouse PK model was utilized from literature to simulate EMB PK[1].

Mouse PK/PD models were developed by incorporating drug effects into a bacterial infection model that describes the infection of *M. tuberculosis* in BALB/c mice (Eq. S1 &Eq. S2). Parameters of the bacterial infection model were re-estimated based on the control data for each drug, to fit the untreated bacterial burden over time for their respective experiment and reliably quantify the drug efficacy separate from the natural infection dynamic (**Table S2**)[2]. The inhibitory effect of the adaptive immune response during the treatment period was investigated with certain assumptions. Plasma concentration was used as the independent variable to describe the treatment response for all mouse PD studies except that of PZA using cumulative AUC in acute and sub-

acute infection model studies due to the time-varying PZA effect being dependent upon the pH of the microenvironment in the phagosomal compartment during the early treatment period which is, itself, a function of the time ($Conc_{PZA} \times \mathrm{d}t$).

PK/PD relationships for drug effect were optimized by fitting the log-transformed mouse PD data to linear, nonlinear, log-linear, E_{max} and sigmoidal functions. A delay effect was added to optimize the relationship between plasma exposures, time and treatment response (Eq. S3 & S4, Figure S2). An additive error model was used to describe residual error for the mouse PK/PD models. Visual predictive checks (VPCs) of 1000 simulations indicated that the observed data were consistently within the 95% prediction interval of the simulated plasma concentrations and bacterial numbers in the final PK and PK/PD models used for translation for each drug (Figure S2).

$$\frac{dB}{dt} = K_g \times B \times \left(1 - \frac{K_B \times B^{\gamma_B}}{B_{50}^{\gamma_B} + B^{\gamma_B}}\right) \times \left(1 - \frac{K_T \times t^{\gamma_T}}{T_{50}{}^{\gamma_T} + t^{\gamma_T}}\right) \quad - K_d \times B \qquad Eq.S1$$

$$\frac{dB}{dt} = K_g \times B \times \left(1 - \frac{K_B \times B^{\gamma_B}}{B_{50}^{\gamma_B} + B^{\gamma_B}}\right) \times \left(1 - \frac{K_T \times t^{\gamma_T}}{T_{50}{}^{\gamma_T} + t^{\gamma_T}}\right) \quad - K_d \times B - EFF \times B \qquad Eq.S2$$

B: bacterial number

t: incubation time since inoculation

K_g: bacterial growth rate

K_d: bacterial natural death rate

K_B: bacterial number-dependent maximal adaptive immune effect

B_{50}: bacterial number that results in half of K_B

γ_B: steepness of bacterial number-dependent immune effect relationship

K_T: incubation time-dependent maximal adaptive immune effect

T_{50}: bacterial number that results half of K_T

γ_T: steepness of time-dependent immune effect relationship

EFF: bacterial killing rate

$$\frac{dA_{\text{delay}}}{dt} = K_{delay} \times \left(\frac{A_2}{V_1} - A_{\text{delay}}\right) \quad Eq.S3$$

A_{delay}: the delayed concentration level associated with drug effect

K_{delay}: the delay rate of the plasma concentration associated with drug effect

$$EFF = \frac{A_{delay}^{\gamma} \times E_{max}}{EC_{50}^{\gamma} + A_{delay}^{\gamma}} \quad Eq.S4$$

E_{max}: the maximal level of drug effect

EC_{50}: the delayed concentration that results in half of the maximal drug effect

γ: the steepness of the relationship between the delayed plasma concentration and drug effect

Clinical PK models were implemented from either published models or developed in NONMEM based on either internal clinical data or extracted literature data (**Table S1)**. Single and multi-compartment PK models were tested for drugs modeled. Linear and nonlinear clearance, absorption and bioavailability were also tested when appropriate. Additive, proportional and combination residual error models were tested for the best fit.

Translational model development for EBA prediction

The outcome of clinical EBA studies was predicted by translating the mouse exposure-response relationships to TB patients. Either average patient covariates or no covariates were included for simulating human PK exposures for each drug. The outcomes of EBA studies were predicted by simulating the CFU counts in the sputum of TB patients based on the translatable PK/PD relationships identified in the mouse efficacy studies. Drug dose was as specified in the

EBA publication, where weight-based dosing was multiplied by the median weight in the studied population and rounded based on available formulations. In the untreated control arm, typically minimal changes occur during the first two days of study (1-8). As such, the net CFU count change rate (K_{net}) during the first two days of study was considered to be 0 and the changes in CFU counts were only driven by the drug effect *(Eq. S5)*.

$$\frac{dB}{dt} = K_{net} \times B - EFF \times B \qquad Eq.S5$$

K_{net}: the net rate of change in bacterial number in the sputum of TB patients

EBA values were calculated as the daily change of CFU counts over specific days with treatment for ten drugs individually. A thousand simulations for predicting clinical studies were conducted for each drug.

Supplemental Results

Mouse PK and PK/PD Model Development

Mouse PK models of nine out of the ten TB drugs, including BDQ, DLM, INH, LZD, MXF, PMD, PZA, RIF and RPT, were developed using plasma concentration data individually, among which partial data for DLM were digitized from a published study (3 mg/kg)[3]. EMB PK was simulated using a published mouse PK model[1]. Either a one-compartment or two-compartment structural model with first-order absorption and linear or non-linear clearance was used to describe the mouse PK data for each drug (Supplementary Figure S1, Table 1) (*Eq. S*6-S11). Saturable bioavailability was incorporated for PMD and RIF PK models *(Eq. S*12).

First-order Absorption model:

$$\frac{dA_1}{dt} = -K_a \times A_1 \quad Eq.S6$$

A_1 is the amount of drug in the gastrointestinal tract absorbed into the systemic circulation

K_a is the first-order absorption rate of the drug

t is the time after the dos

One-compartment PK model:

$$\frac{dA_2}{dt} = K_a \times A_1 - K_e \times A_2 \quad Eq.S7$$

A_2 is the amount of drug in the central compartment

K_e is the elimination rate of the drug from the central compartment

Two-compartment PK model:

$$\frac{dA_2}{dt} = K_a \times A_1 - K_e \times A_2 - \frac{Q}{V_1} \times A_2 + \frac{Q}{V_2} \times A_3 \quad Eq.S8$$

$$\frac{dA_3}{dt} = \frac{Q}{V_1} \times A_2 - \frac{Q}{V_2} \times A_3 \quad Eq.S9$$

A_3 is the amount of drug in the peripheral compartment

Q is the intercompartmental clearance

V_1 is the volume of the central compartment

V_2 is the volume of the peripheral compartment

Linear clearance:

$$K_e = \frac{CL}{V_1} \quad Eq.S10$$

CL is the clearance, which is defined as the volume of plasma completely cleared of a drug per unit time

Non-linear clearance:

$$K_e = \frac{K_m \times CL_{in}}{\left(K_m + \frac{A_2}{V_1}\right) \times V_1} \quad Eq.S11$$

V_{max} is the maximal clearance, which is defined as the maximal volume of plasma completely cleared of a drug per unit time

K_m is the concentration of drug that results in half of the maximal clearance

CL_{in} is the ratio between Vmax and Km.

Saturable bioavailability:

$$F = 1 - \frac{F_{DIF} \times (Dose - Dose_{ref})}{Dose - Dose_{ref} + FD_{50}} \qquad Eq.S12$$

F: the extent of drug absorbed from oral dosing compartment into systemic compartment

F_{DIF}: the maximum difference in bioavailability from 100% (bound between 0% and 100%)

$Dose_{ref}$: the reference dose that has 100% bioavailability

FD_{50}: the dose achieving half maximal reduction in bioavailability

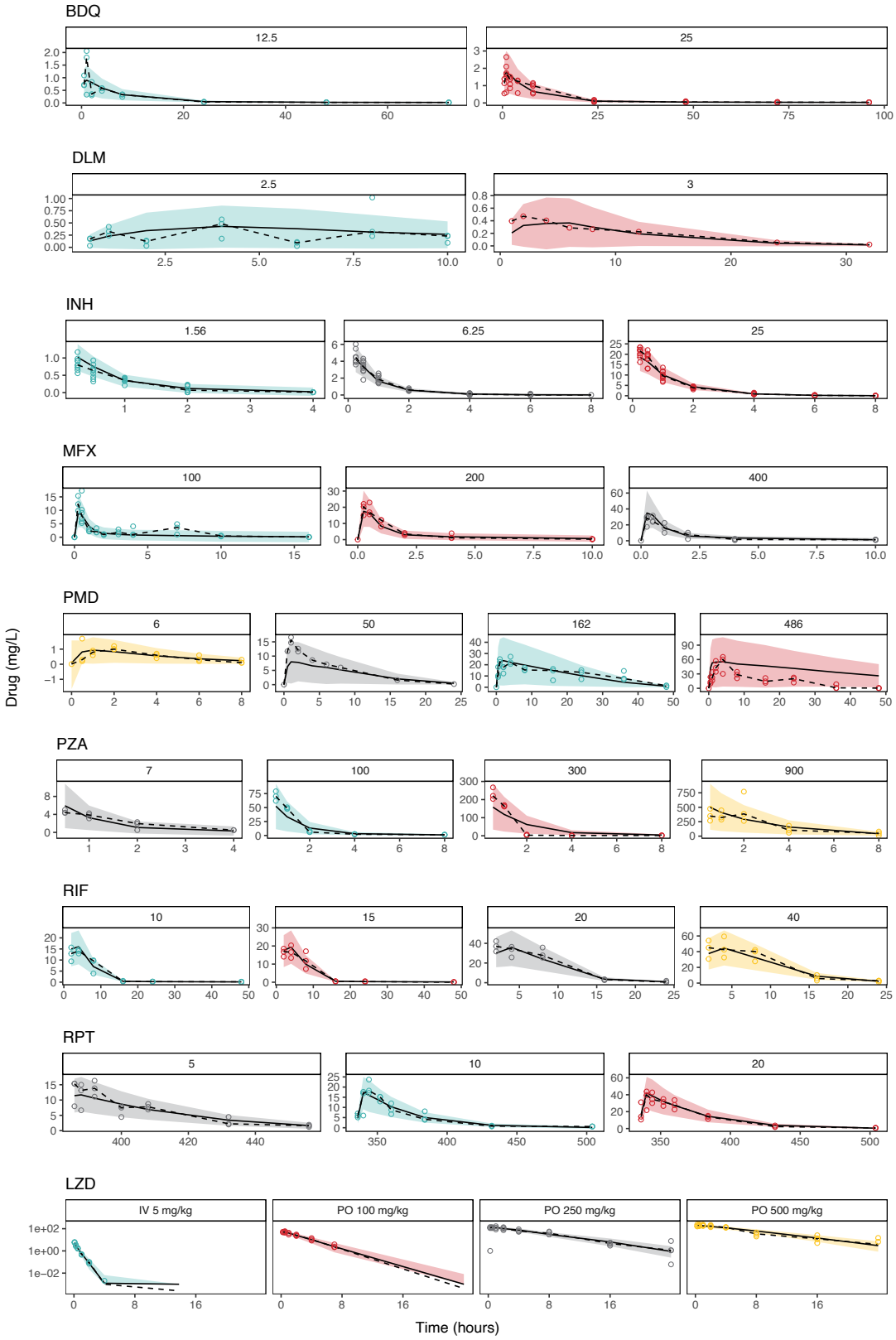

Figure S1 Visual predictive checks for final mouse PK models at representative doses. All doses are in mg/kg and orally administered unless otherwise state

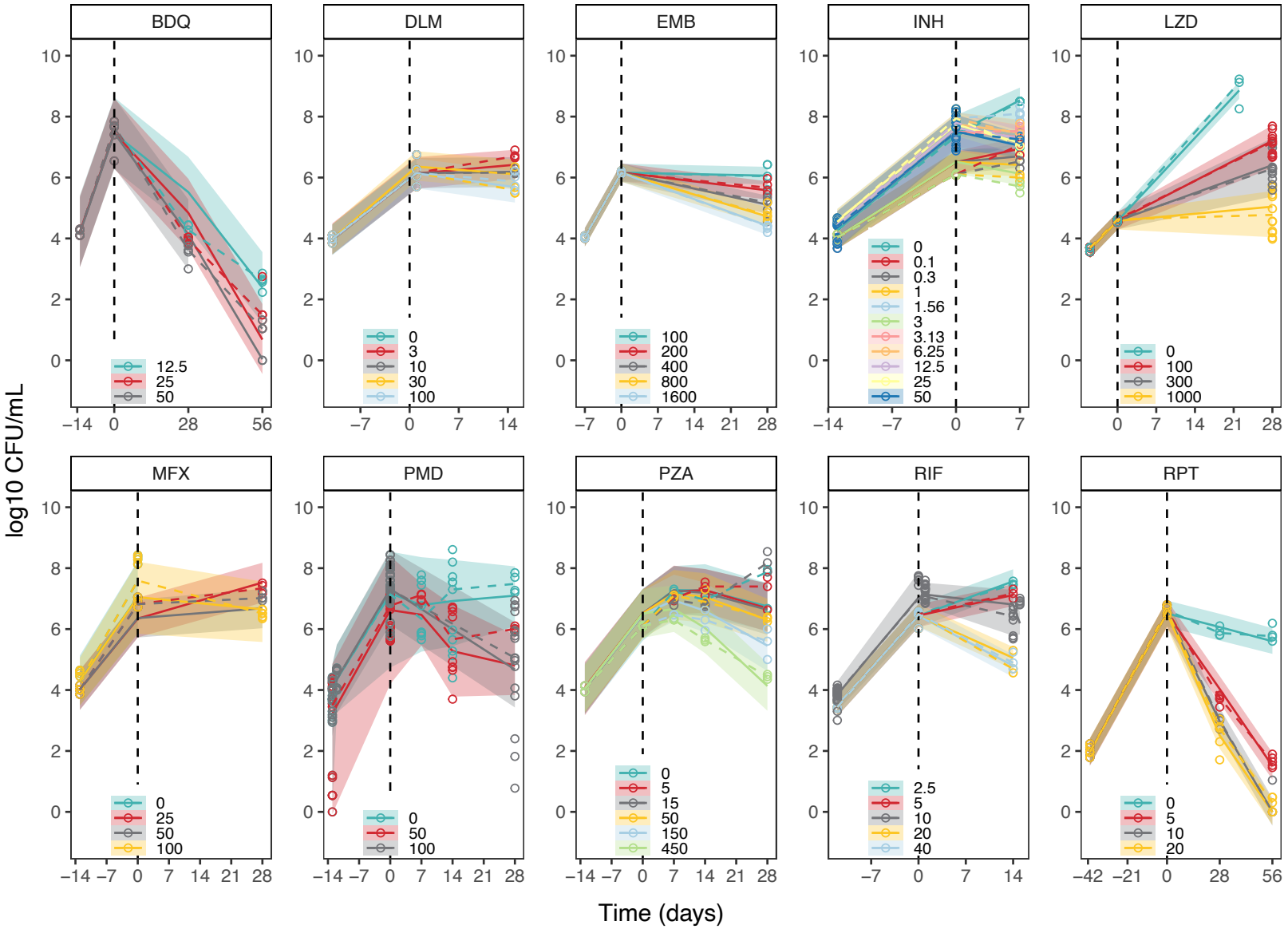

Figure S2 **Visual predictive checks for final mouse PD models at representative doses.** All doses are in mg/kg and orally administered.

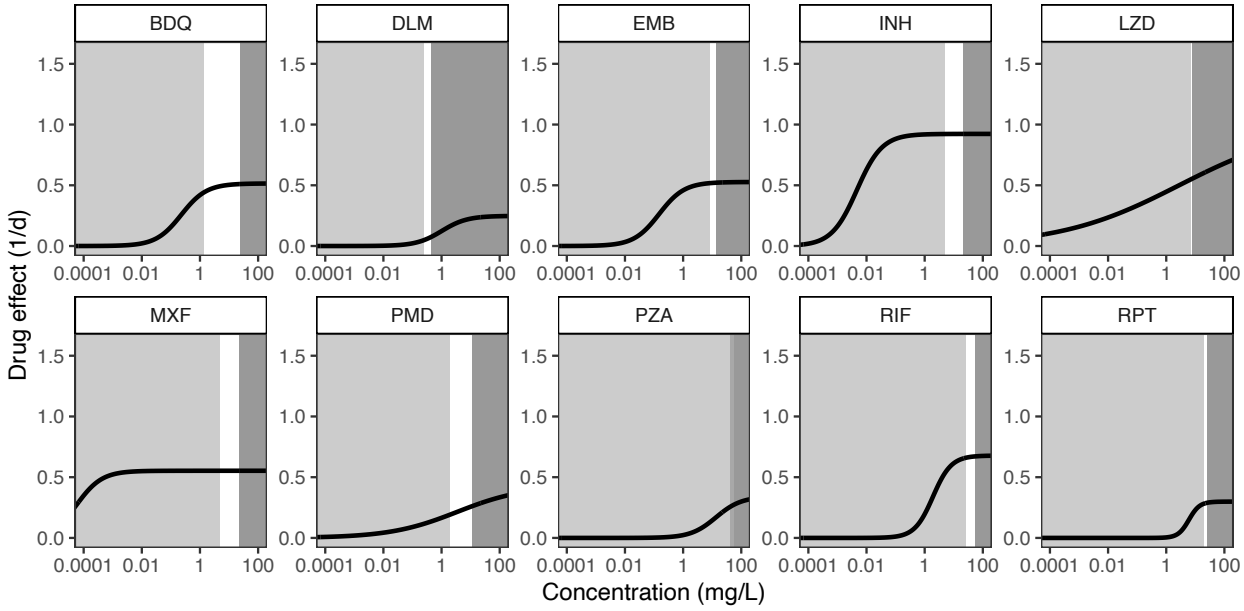

Figure S3 Comparison between human PK concentrations reached at clinical dose levels (light grey), upper limits of drug concentrations within safety ranges (dark grey) and concentration-response relationships for ten TB drugs. Upper limits of clinical dose levels were defined as concentrations up to the C_{max}. Lower limits of safety ranges were defined as the C_{max} of the maximum tolerated dose tested in humans.

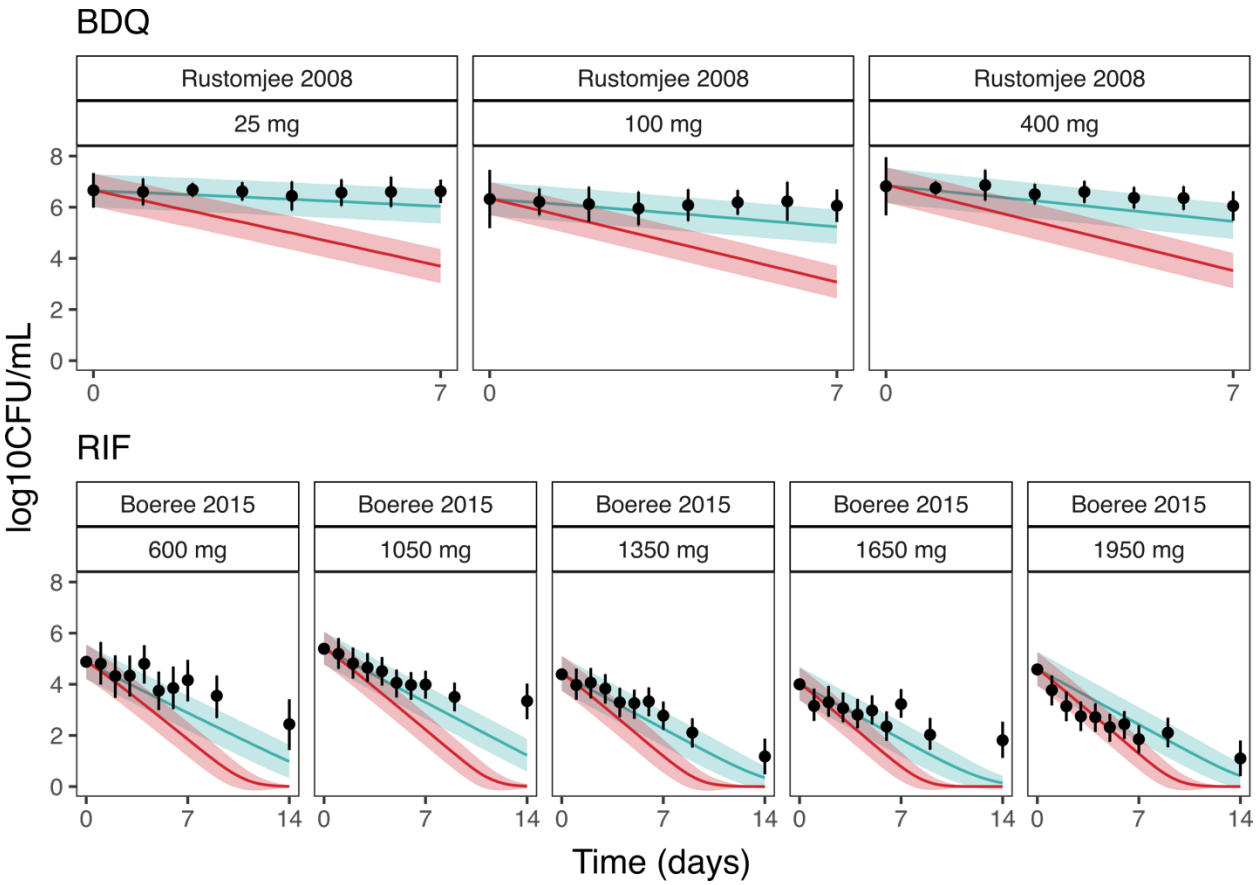

Figure S4 The immune component of the model-based translational platform is essential for accurate prediction of early bactericidal activity. Comparison of prediction of sputum CFU counts in TB patients during treatment with bedaquiline (BDQ) and rifampin (RIF) at multiple dose levels using PKPD relationships from mathematical models when immune effect (imm) is accounted for and not accounted for.

Table S1 Mouse and human PK and PD database of ten TB drugs.

Mouse PK

PK data	BDQ	DLM	EMB	INH	LZD	MXF	PMD	PZA	RIF	RPT
Observations	90	29	186	153	238	74	215	100	66	69
Doses (mg/kg)	12.5, 25, single dose	2.5, 3 single dose	10, 16, 30, 100, 300, 1000 mg/kg	1.56, 6.25, 25, single dose	3*, 5*, 100, 250, 500 single dose	100, 200, 400 daily for 32 days	6, 9, 12,18, 28.8,50,54, 162, 486 single dose; 100 daily for 4 or 8 weeks	7, 22, 100, 300, 600, 900, single dose	10, 15, 20, 40, daily for 2 weeks	5, 10, 20, daily for 16 days
Data Source	JHU[4]	JHU[5] and published data[3]	Published data[1]	JHU[6–9]	JHU[7] & TBA	JHU[8]	JHU[5]	JHU[4,9]	JHU[7,9,10]	JHU[10]
Protein binding($f_{u,\ Human/Mouse}$)	1.0 [11]	1.0 [12]	1.0*	1.455 [13,14]	0.986 [15,16]	0.797 [17]	0.99 [18]	0.925 [19] (mouse data JHU unpublished)	4.545 [13,20]	0.422 [21,22]

*personal communication

Mouse PD

PD data	BDQ	DLM	EMB	INH	LZD	MXF	PMD	PZA	RIF	RPT
Animal	Mouse	Mouse	Mouse	Mouse	Mouse	Mouse	Mouse	Mouse	Mouse	Mouse
Observations	57	56	54	414	261	63	283	84	203	75
Doses (mg/kg)	12.5, 25, 50	3,10,30,100	100, 200, 400, 800, 1600	0.1, 0.3, 1, 1.56, 3, 3.13, 6.25, 10, 12.5, 25, 30, 50, 100	7.2, 10, 20, 21.4, 30, 40, 60, 72, 100, 200, 300, 335, 1000	25, 50, 100	50, 100	3, 5, 10, 15, 25, 30, 37.5, 50, 75, 100, 150, 300, 450, 600, 900	2.5, 5, 10, 20, 40, 80, 160, 320, 640	5, 10, 20
Treatment duration (days)	70	56	28	21-56	28	28-56	14-28	28-56	14-56	56

Data Source	JHU[4]	JHU[5] and published data[3]	JHU	JHU[6–9]	JHU[7] & TBA	JHU[8]	JHU[5]	JHU[4,9]	JHU[7,9,10]	JHU[10]

Human PK

Drugs	PK Structure Model	Doses	No. of Patients / Samples	References
BDQ	3-cmt model with transit absorption	400 mg p.o. daily for 14 days and 200 mg p.o. three times per week for 24 weeks	335 / 2,843	[23]
DLM	2-cmt with linear absorption and saturable bioavailability	100, 200, 300, 400 mg p.o. daily for 14 days	744 / 20,483	[24]
EMB	2-cmt with transit absorption and clearance	800, 1000, 1200, 1500 mg p.o. 5 days/week for ≥4 weeks	189 / 1,869	[25]
INH	2-cmt PK model with linear absorption and clearance	100, 225, 240, 300 and 400 mg p.o. daily, 5 days/week for 2 weeks; 200, 300 and 450 mg p.o.daily, 7 days/week for 1 week	235 / 2,352	[26]
LZD	2-cmt with non-linear clearance	300 mg, 600 mg or 1200 mg p.o. for 6 months	104 / 497	[27]
MXF	2-cmt with transit absorption and linear clearance	400 mg p.o. daily for 7 days	241 / 856	[28]
PMD	1-cmt model with transit absorption and dose-dependent absorption, bioavailability, and volume	200, 600, 1000, 1200 mg p.o. daily for 14 days	1,054 / 17,725	[29]
PZA	1-cmt PK model with first order absorption and clearance	1200, 1500 and 2000 mg p.o. daily, 5 days/week for 2 weeks; 1000, 1500 and 2000 mg p.o. daily 7 days/week for 2 months	227 / 3,092	[30]
RIF	1-cmt PK model (saturable bioavailability and elimination, transit absorption and auto-induction)	10, 20, 25, 30, 35, or 40 mg/kg p.o. daily over 2 weeks	83 / 913	[31]

RPT	1-cmt PK model (saturable bioavailability, transit absorption and auto-induction)	300, 450, 600, 750, 900, 1050, 1200, 1350, 1500, 1650, 1800 mg p.o. once weekly up to twice daily for up to four months	863 / 4,388	[32]

Human EBA studies

Drugs	Doses	Baseline (log_{10} CFU/mL)	References
BDQ	100, 200, 300 and 400 mg (with 200, 400, 500, 700 mg loading dose on first day and 100, 300, 400, 500 mg on second day, respectively)	6.302 (100 mg), 6.001 (200 mg), 6.071 (300 mg), 6.625 (400 mg)	[33,34]
	25, 100, 400 mg	6.66 (25 mg), 6.32 (100 mg), 6.82 (400 mg)	
DLM	100, 200, 300 and 400 mg	7.06 (100 mg), 6.75 (200 mg), 6.72 (300 mg), 6.82 (400 mg)	[35]
EMB	15, 25, and 50 mg/kg	6.92	[36]
INH	9, 18.75, 37.5, 75, 150, 300 and 600 mg	6.491 (9 mg), 6.585 (18.75 mg), 7.169 (37.5 mg), 7.031 (75 mg), 7.115 (150 mg), 6.504 (300 mg), 6.995 (600 mg)	[37]
LZD	600 mg QD, 600 mg BD	6.34 (600 mg QD), 6.44 (600 mg BD)	[38]
MXF	400 mg	6.19 (400 mg Johnson), 7.15 (400 mg Pletz), 7.23 (400 mg Gosling)	[39–41]
PMD	50, 100, 150, 200, 600, 1000, 1200 mg	6.1 (50 mg), 5.8 (100 mg), 6 (150 mg), 6.1 (200 mg Diacon 2012), 6.592 (200 mg Diacon 2010), 6.335 (600 mg), 6.309 (1000 mg), 6.057 (1200 mg)	[42,43]
PZA	1500, 2000 mg	5.56 (1500mg), 6.910 (2000mg)	[36,44]
RIF	10, 20, 25, 30 and 35 mg/kg	4.88 (10 mg/kg), 4.00 (20 mg/kg), 5.39 (25 mg/kg), 4.58 (30 mg/kg), 4.39 (35 mg/kg)	[20]
RPT	300, 600, 900, 1200 mg	N/A	[45]

*intravenous dosing

Table S2 Final parameters for the bacterial infection model[46] for each drug based on the control data.

Parameter	BDQ	DLM	EMB	INH	LZD	MXF	PMD	PZA	RIF	RPT
K_g (day^{-1}) ($\leq$ 4 days)	0.509	0.370	1.11	0.512	0.845	0.461	0.423	0.512	0.512	0.509
K_g (day^{-1}) (> 4 days)	1.2	0.88104	1.11	1.2168	1.50968	1.1055	1.1935	1.2168	1.2168	1.11
K_d (day^{-1})	0.41	0.41	0.41	0.41	0.41	0.41	0.41	0.41	0.41	0.41
K_B (%)	23.695	28.511	20.3	24.174	39	27.478	68.937	24.174	24.174	23.695
B_{50} ($\log_{10}$ CFU)	6.9914	7.0241	7.86	7.0512	8.3385	6.9136	7.7610	7.0512	7.0512	6.9914
γ_B	2.3276	1.2316	0.203	2.1939	2.9	1.7883	0.20574	2.1939	2.1939	2.3276
K_T (%)	66.4	64.722	70.2	66.319	69.6	65.15	63.763	66.319	66.319	66.4
T_{50} (day)	19.308	19.725	17.4	19.33	17.5	19.602	18.816	19.33	19.33	19.308
γ_T	5.5277	5.7879	0.702	5.3599	5.13	5.5605	5.7651	5.3599	5.3599	5.5277

B_{50} = CFU counts to reach half of K_B, BDQ = bedaquiline, CFU = colony forming units, DLM = delamanid, EMB = ethambutol, INH = isoniazid, K_g = bacterial growth rate, K_d = bacterial death rate, KB = bacterial inhibitory CFU-dependent adaptive immune effect, K_T = bacterial inhibitory time-dependent adaptive immune effect, LZD = linezolid, MXF = moxifloxacin, PMD = pretomanid, PZA = pyrazinamide, RIF = rifampin, RPT = rifapentine, T_{50} = time to reach half of maximal time covariate, γ_B = steepness of the CFU-dependent adaptive immune effect curve, γ_T = steepness of the CFU-dependent adaptive immune effect curve

References

1. Chen, C., Ortega, F., Alameda, L., Ferrer, S. & Simonsson, U. S. H. Population pharmacokinetics, optimised design and sample size determination for rifampicin, isoniazid, ethambutol and pyrazinamide in the mouse. *Eur. J. Pharm. Sci.* **93**, 319–333 (2016).
2. Zhang, N. *et al.* Mechanistic Modeling of Mycobacterium tuberculosis Infection in Murine Models for Drug and Vaccine Efficacy Studies. *Antimicrob. Agents Chemother.* **64**, (2020).
3. Sasahara, K. *et al.* Pharmacokinetics and Metabolism of Delamanid, a Novel Anti-Tuberculosis Drug, in Animals and Humans: Importance of Albumin Metabolism In Vivo. *Drug Metab. Dispos.* **43**, 1267–1276 (2015).
4. Irwin, S. M. *et al.* Bedaquiline and Pyrazinamide Treatment Responses Are Affected by Pulmonary Lesion Heterogeneity in Mycobacterium tuberculosis Infected C3HeB/FeJ Mice. *ACS Infect Dis* **2**, 251–267 (2016).
5. Tasneen, R. *et al.* Contribution of the nitroimidazoles PA-824 and TBA-354 to the activity of novel regimens in murine models of tuberculosis. *Antimicrob. Agents Chemother.* **59**, 129–135 (2015).
6. Tyagi, S. *et al.* Bactericidal activity of the nitroimidazopyran PA-824 in a murine model of tuberculosis. *Antimicrob. Agents Chemother.* **49**, 2289–2293 (2005).
7. Bigelow, K. M. *et al.* Pharmacodynamic Correlates of Linezolid Activity and Toxicity in Murine Models of Tuberculosis. *J. Infect. Dis.* **223**, 1855–1864 (2021).
8. Yoshimatsu, T. *et al.* Bactericidal activity of increasing daily and weekly doses of moxifloxacin in murine tuberculosis. *Antimicrob. Agents Chemother.* **46**, 1875–1879 (2002).

9. Almeida, D. *et al.* Paradoxical effect of isoniazid on the activity of rifampin-pyrazinamide combination in a mouse model of tuberculosis. *Antimicrob. Agents Chemother.* **53**, 4178–4184 (2009).
10. Rosenthal, I. M. *et al.* Daily dosing of rifapentine cures tuberculosis in three months or less in the murine model. *PLoS Med.* **4**, e344 (2007).
11. Committee for Medicinal Products for Human Use (CHMP). *CHMP assessment report SIRTURO*. https://www.ema.europa.eu/en/documents/variation-report/sirturo-h-c-2614-ii-0033-g-epar-assessment-report_en.pdf (2019).
12. Shimokawa, Y. *et al.* Metabolic Mechanism of Delamanid, a New Anti-Tuberculosis Drug, in Human Plasma. *Drug Metab. Dispos.* **43**, 1277–1283 (2015).
13. Woo, J. *et al.* In vitro protein binding characteristics of isoniazid, rifampicin, and pyrazinamide to whole plasma, albumin, and alpha-1-acid glycoprotein. *Clin. Biochem.* **29**, 175–177 (1996).
14. Jayaram, R. *et al.* Isoniazid pharmacokinetics-pharmacodynamics in an aerosol infection model of tuberculosis. *Antimicrob. Agents Chemother.* **48**, 2951–2957 (2004).
15. Lepak, A. J., Marchillo, K., Pichereau, S., Craig, W. A. & Andes, D. R. Comparative pharmacodynamics of the new oxazolidinone tedizolid phosphate and linezolid in a neutropenic murine Staphylococcus aureus pneumonia model. *Antimicrob. Agents Chemother.* **56**, 5916–5922 (2012).
16. Dryden, M. S. Linezolid pharmacokinetics and pharmacodynamics in clinical treatment. *J. Antimicrob. Chemother.* **66**, iv7–iv15 (2011).

17. Siefert, H. M. *et al.* Pharmacokinetics of the 8-methoxyquinolone, moxifloxacin: a comparison in humans and other mammalian species. *J. Antimicrob. Chemother.* **43 Suppl B**, 69–76 (1999).
18. Rakesh *et al.* Synthesis and evaluation of pretomanid (PA-824) oxazolidinone hybrids. *Bioorg. Med. Chem. Lett.* **26**, 388–391 (2016).
19. Stada Pharmaceuticals,Inc, Cranbury, NJ, 2004. Product Information: pyrazinamide oral tablets, pyrazinamide oral tablets. Preprint at https://www.micromedexsolutions.com/micromedex2/librarian/CS/E2AC9E/ND_PR/evidencexpert/ND_P/evidencexpert/DUPLICATIONSHIELDSYNC/C17097/ND_PG/evidencexpert/ND_B/evidencexpert/ND_AppProduct/evidencexpert/ND_T/evidencexpert/PFActionId/evidencexpert.DoIntegratedSearch?SearchTerm=pyrazinamide&UserSearchTerm=pyrazinamide&SearchFilter=filterNone&navitem=searchALL#cite5_dp.
20. de Steenwinkel, J. E. M. *et al.* Optimization of the rifampin dosage to improve the therapeutic efficacy in tuberculosis treatment using a murine model. *Am. J. Respir. Crit. Care Med.* **187**, 1127–1134 (2013).
21. sanofi-aventis U.S. (per manufacturer), Bridgewater, NJ, 2014. Product Information: PRIFTIN(R) oral tablets, rifapentine oral tablets. Preprint at https://www.micromedexsolutions.com/micromedex2/librarian/CS/A32D19/ND_PR/evidencexpert/ND_P/evidencexpert/DUPLICATIONSHIELDSYNC/0EBD73/ND_PG/evidencexpert/ND_B/evidencexpert/ND_AppProduct/evidencexpert/ND_T/evidencexpert/PFActionId/evidencexpert.DoIntegratedSearch?SearchTerm=rifapentine&UserSearchTerm=rifapentine&SearchFilter=filterNone&navitem=searchALL#cite2_dp.

22. Assandri, A., Ratti, B. & Cristina, T. Pharmacokinetics of rifapentine, a new long lasting rifamycin, in the rat, the mouse and the rabbit. *J. Antibiot.* **37**, 1066–1075 (1984).
23. Svensson, E. M., Dosne, A.-G. & Karlsson, M. O. Population Pharmacokinetics of Bedaquiline and Metabolite M2 in Patients With Drug-Resistant Tuberculosis: The Effect of Time-Varying Weight and Albumin. *CPT Pharmacometrics Syst Pharmacol* **5**, 682–691 (2016).
24. Wang, X., Mallikaarjun, S. & Gibiansky, E. Population Pharmacokinetic Analysis of Delamanid in Patients with Pulmonary Multidrug-Resistant Tuberculosis. *Antimicrob. Agents Chemother.* **65**, (2020).
25. Jönsson, S. *et al.* Population pharmacokinetics of ethambutol in South African tuberculosis patients. *Antimicrob. Agents Chemother.* **55**, 4230–4237 (2011).
26. Wilkins, J. J. *et al.* Variability in the population pharmacokinetics of isoniazid in South African tuberculosis patients. *Br. J. Clin. Pharmacol.* **72**, 51–62 (2011).
27. Imperial, M. Z., Nedelman, J. R., Conradie, F. & Savic, R. M. Proposed Linezolid Dosing Strategies to Minimize Adverse Events for Treatment of Extensively Drug-Resistant Tuberculosis. *Clin. Infect. Dis.* **74**, 1736–1747 (2021).
28. Zvada, S. P. *et al.* Moxifloxacin population pharmacokinetics and model-based comparison of efficacy between moxifloxacin and ofloxacin in African patients. *Antimicrob. Agents Chemother.* **58**, 503–510 (2014).
29. Salinger David H., Subramoney Vishak, Everitt Daniel & Nedelman Jerry R. Population Pharmacokinetics of the Antituberculosis Agent Pretomanid. *Antimicrob. Agents Chemother.* **63**, e00907-19 (2019).

30. Wilkins, J. J. *et al.* Variability in the population pharmacokinetics of pyrazinamide in South African tuberculosis patients. *Eur. J. Clin. Pharmacol.* **62**, 727–735 (2006).
31. Svensson, R. J. *et al.* A Population Pharmacokinetic Model Incorporating Saturable Pharmacokinetics and Autoinduction for High Rifampicin Doses. *Clin. Pharmacol. Ther.* **103**, 674–683 (2018).
32. Hibma, J. E. *et al.* Rifapentine Population Pharmacokinetics and Dosing Recommendations for Latent Tuberculosis Infection. *Am. J. Respir. Crit. Care Med.* **202**, 866–877 (2020).
33. Diacon, A. H. *et al.* Randomized dose-ranging study of the 14-day early bactericidal activity of bedaquiline (TMC207) in patients with sputum microscopy smear-positive pulmonary tuberculosis. *Antimicrob. Agents Chemother.* **57**, 2199–2203 (2013).
34. Rustomjee, R. *et al.* Early bactericidal activity and pharmacokinetics of the diarylquinoline TMC207 in treatment of pulmonary tuberculosis. *Antimicrob. Agents Chemother.* **52**, 2831–2835 (2008).
35. Diacon, A. H. *et al.* Early bactericidal activity of delamanid (OPC-67683) in smear-positive pulmonary tuberculosis patients. *Int. J. Tuberc. Lung Dis.* **15**, 949–954 (2011).
36. Jindani, A., Aber, V. R., Edwards, E. A. & Mitchison, D. A. The early bactericidal activity of drugs in patients with pulmonary tuberculosis. *Am. Rev. Respir. Dis.* **121**, 939–949 (1980).
37. Donald, P. R. *et al.* The early bactericidal activity of isoniazid related to its dose size in pulmonary tuberculosis. *Am. J. Respir. Crit. Care Med.* **156**, 895–900 (1997).
38. Dietze, R. *et al.* Early and extended early bactericidal activity of linezolid in pulmonary tuberculosis. *Am. J. Respir. Crit. Care Med.* **178**, 1180–1185 (2008).

39. Gosling, R. D. *et al.* The bactericidal activity of moxifloxacin in patients with pulmonary tuberculosis. *Am. J. Respir. Crit. Care Med.* **168**, 1342–1345 (2003).

40. Johnson, J. L. *et al.* Early and extended early bactericidal activity of levofloxacin, gatifloxacin and moxifloxacin in pulmonary tuberculosis. *Int. J. Tuberc. Lung Dis.* **10**, 605–612 (2006).

41. Pletz, M. W. R. *et al.* Early bactericidal activity of moxifloxacin in treatment of pulmonary tuberculosis: a prospective, randomized study. *Antimicrob. Agents Chemother.* **48**, 780–782 (2004).

42. Diacon, A. H. *et al.* Early bactericidal activity and pharmacokinetics of PA-824 in smear-positive tuberculosis patients. *Antimicrob. Agents Chemother.* **54**, 3402–3407 (2010).

43. Diacon, A. H. *et al.* Phase II dose-ranging trial of the early bactericidal activity of PA-824. *Antimicrob. Agents Chemother.* **56**, 3027–3031 (2012).

44. Diacon, A. H. *et al.* Bactericidal activity of pyrazinamide and clofazimine alone and in combinations with pretomanid and bedaquiline. *Am. J. Respir. Crit. Care Med.* **191**, 943–953 (2015).

45. Sirgel, F. A. *et al.* The early bactericidal activities of rifampin and rifapentine in pulmonary tuberculosis. *Am. J. Respir. Crit. Care Med.* **172**, 128–135 (2005).

46. Zhang Nan *et al.* Mechanistic Modeling of Mycobacterium tuberculosis Infection in Murine Models for Drug and Vaccine Efficacy Studies. *Antimicrob. Agents Chemother.* **64**, e01727-19 (2020).